USING FLUORESCEIN AS A FLUOROPHORE TO TEST UV AND LIGHT PENETRATION OF FLOCCULATED PARTICLES

S.A.D.A Nilakshi Dissanayake, Michael J Cree, Mark Lay, Lee Streeter, Graeme D.E. Glasgow

School of Enginnering, The University of Waikato

ABSTRACT

UV disinfection is commonly used in water treatment to inactivate pathogens such as cryptosporidium and viruses for preventing diseases such as cryptosporidiosis and norovirus in communities. Disinfection typically follows water treatment steps such as coagulation, flocculation, clarification, and filtration. However, particles in water, for example a floc 0.1 to 100 μm in diameter, made from humic and inorganic substances present in the water, surrounding a cryptosporidium oocyst or virus, can protect the pathogens from UV exposure. While water treatment steps prior to disinfection remove 99% of the particulates, particles can still be present in the 1000's to 10,000's per litre after filtration. While typically the chances of a floc particle carrying a virus or oocyst might be low, in some regions, particularly during calving in the dairy industry, oocyst concentrations in the water might be high due to cryptosporidiosis in calves. Therefore, it is useful to test the properties of the floc compound for UV penetration to determine if the method of disinfection is appropriate.

This study examines UV and visible light penetration of humic and kaolin floc using fluorescein as a fluorophore. Kaolin and humic samples were prepared in 20, 40, 60, 80 and 100 mg/L concentrations 400 ml of each sample was dosed 200 μl of 1 mg/ml fluorescein and coagulated by adding enough $Al_2(SO_4)_3$ so the solution had a zero zeta-potential. Flocculation was carried out in a jar tester apparatus by mixing at 100 rpm for 2 minutes, slow mixing at 30 rpm for 5 minutes, and settling for 5 minutes. Floc was also prepared using the same method using 400 ml aliquots of 60 mg/L kaolin, dosing with 50, 100, 200, 300 μl of 1 mg/ml fluorescein. After settling, water samples were measured for turbidity, pH, samples containing the floc for fluorescence intensity using a fluorescence spectrophotometer and particle size under the microscope.

Fluorescence was observed at the 260 nm and 490 nm excitation wavelengths, with fluorescence emissions around the 510 nm wavelength. Fluorescence intensity decreased with increased kaolin and humic concentration, but the intensity could be increased by increasing the dose of fluorescein. At the lower

doses of fluorescein and higher concentrations of humic and kaolin, first and second order refraction in the excitation emission matrix was observed which was due to the diffraction grating of the instrument and intensified its excitation light reflecting off the particles rather than being absorbed by the fluorescein. To prevent this from happening, a 400 ml sample containing 20 mg/L kaolin required 333 µl of 1 mg/L fluorescein, a kaolin to fluorescein mass ratio of 60:1. Turbidity increased with increased humic and kaolin concentrations and pH was maintained in the range of 6 to 7. Particle size ranged from 20 to 315 µm, and the particles were a mixture of spherical and non-spherical shapes.

KEYWORDS

Fluorescence intensity, excitation emission matrix, UV penetration, floc properties

PRESENTER PROFILE

Nilakshi Dissanayake received B.Tech. (Eng.) (Hons.) degree in electronics and communications engineering and M.Phil degree from The Open University of Sri Lanka. Her research interest includes sensor developments for environment applications. Currently she is pursuing a PhD degree at the University of Waikato.

INTRODUCTION

In large scale water treatment plants, chemical oxidation processes, membrane filtering and UV disinfection are used to remove and inactivate pathogens in water (LeChevallier and Au, 2004). UV light in the wavelength range of 200 to 300 nm inactivates the replication of microorganisms by damaging their nucleic acids in their DNA and RNA (USEPA, 2010). UV disinfection is commonly used to treat cryptosporidium and viruses to prevent diseases such as cryptosporidiosis and norovirus in communities (Rossle and Latif, 2013; Augsburger et al.,2021). Water treatment steps prior to disinfection remove the majority of the particulates, which reduces the possibility of a virus or oocyst being carried by a floc particle. However, there can be thousands of particles in 1 L in the µm size range even after filtration. In addition, during the calving season in the regions with dairy industries, oocyst concentration might increase due to cryptosporidiosis in calves. Hence, particles in water can coagulate with cysts or oocysts, viruses during the water treatment process and can protect pathogens from UV disinfection. Efficiency of UV disinfection is reduced with organic particle size less than 2 µm according to the study of Templeton et al. (2005). Research by Cantwell and Hofmann (2008) state that expose of low-pressure UV light is incapable of inactivating coliform bacteria protected by particles as small as 11 µm. Further, Kollu and Örmeci (2012), mentioned aggregated *Escherichia coli* (*E. coli*) and particle sizes larger than 25 µm reduces the inactivation of *E. coli*. Particle size may also vary with the type of microorganism that is protected by the particles.

In water, biological contaminants and particles such as humic and inorganic substances are present in different sizes in the range of 0.1 to 100 µm (Gregory,

2005). Particles can aggregate in different forms and shapes due to water properties such as pH, turbidity, and particle size. This makes it difficult to analyze the influence of particles and their ability to protect viruses and oocysts in water. In addition, organic and inorganic particulate compounds have different UV absorption properties that limit the UV exposure the microorganism might experience in the particle or scatter light to reduce UV exposure a particular particle might experience. Templeton (2008) reports inorganic particles such as kaolin do not protect pathogens from UV, however the UV absorption of organic particles such as humic and sludge protect pathogens from UV. A model was developed by Emrick et al. (2000) to estimate the required UV exposure to inactivate coliform bacteria in a particle in wastewater secondary effluent. This model has been tested only for coliform bacteria and UV dose and particle size can be modelled accurately only if the inactivation rate and total number of particles in the sample are known. There are many different parameters involved in estimating UV dose required to inactivate different pathogens. Hence, studying UV and light penetration via floc might help in determining if the methods used for disinfection are appropriate.

The use of fluorophore to study different compounds of floc is a hazard free mechanism and an alternative to the experiments with protozoa and viruses. Fluorophores are capable of absorbing energy and re-emit in longer wavelength than the excited wavelength (Lakowicz, 2006). There have been recent developments of fluorescent probes to detect different pathogens in environmental and medical studies (Key et al., 2009, Singh et al.,2016). Fluorescent microparticles were substituted as Cryptosporidium parvum to test the efficiency of a metallic membrane in drinking water treatment (Li et al., 2019). Pang (2009) used modified microspheres to study pathogen transport in ground water. These modifications help to simulate the environment required to observe the particle behavior that helps understand parameters affecting the UV disinfection.

There are different phenomena that take place as light hits the particles. Particles tend to absorb, scatter, reflect and transmit light according to the characteristics of the organic and inorganic compounds that make up the particle. This study focuses on using a fluorophore to measure the UV and light penetration of floc made from kaolin and humic acid and its effect on flocculation, turbidity, particle size and pH.

METHODOLOGY

MATERIAL AND METHODS

Humic acid, kaolin, aluminium sulphate, sodium hydroxide, monobasic potassium phosphate, disodium phosphate, sodium bicarbonate, and fluorescein were supplied by Sigma Aldrich.

1 g/L fluorescein solution was prepared with distilled water in a 100 mL volumetric flask. 50 mg of sodium bicarbonate was added to improve the solubility of fluorescein and the volumetric flask was mixed until the fluorescein was dissolved prior to topping up to the final volume with distilled water. The resulting solution was stored in a brown shott bottle at room temperature.

2-L stock solutions of humic acid and kaolin were prepared at 0.5 g/L and 1 g/L concentrations. A 1-L, 1 g/L aluminium sulphate ($Al_2(SO_4)_3$) solution and a 5-L 0.02M phosphate buffer solution (pH 7) was also prepared by adding 5.8 g KH_2PO_4 (anhydrous) and 8.2 g Na_2HPO_4 (anhydrous) and adjusting to pH 7 using 1 M NaOH solution. The stock solutions of humic acid and kaolin were then diluted to 20, 40, 60, 80 and 100 mg/L concentrations, 2.5 L of each, unbuffered using distilled water and buffered using phosphate buffer.

The zeta potential of each unbuffered humic acid and kaolin solution at each concentration was measured by adding 10 mL of solution to a Mutek Particle Charge Detector (PCD 03) and measuring the zeta potential in mV. The zeta potential was then reduced to zero by gradually adding 50 μl aliquots of aluminium sulphate solution and noting the total volume of alum solution used. The PCD was cleaned between each sample. The volume of alum used to reduce the zeta potential to zero for a 10 mL was scaled up to 400 mL samples of each humic acid and kaolin concentration for conducting flocculation experiments using a Boltac jar tester (Coagulation and flocculation simulator).

For each flocculation experiment, 400 ml of each humic acid and kaolin solution at each concentration was added to the jar tester, followed by addition of 0.2 mL of the 1 g/L fluorescein solution and the required volume of alum solution. The mixtures were rapid-mixed at 100 rpm for 2 minutes, then slow-mixed at 30 rpm for 5 minutes and allowed to settle for 5 minutes. The resulting solution was tested for pH using a Eutech pH150 Meter, turbidity using a 2100P Hach, floc particle size was analysed using a Malvern master particle sizer 3000, and floc morphology using an Olympus BX53 light microscope. 10 ml of each solution was also collected from the 200 ml mark for excitation emission matrix (EEM) fluorescence measurements using a Fluorescence spectrometer (F7000) 3D scan. The fluorescence was measured by exciting the samples in the 250 to 580 nm excitation band in 10 nm increments and measuring the emission in the 470 nm to 580 nm band, also in 10 nm increments.

In a second set of experiments, 400 ml solutions of 60 mg/L humic acid and 60 mg/L kaolin were mixed with different volumes of 1 g/L fluorescein solution, so each solution had final fluorescein concentrations of 0.00, 0.12, 0.24, 0.48, 0.72

and 0.96 mg/L. The flocculation experiments were carried out as described in the previous paragraph and the same tests on the resulting solutions were conducted. In addition, 40 ml of each flocculated solution was collected in 50 mL falcon tubes and centrifuged at 9000 rpm and at a temperature of 4 ^{o}C for 20 minutes. The supernatant was separated and the pellet was refrigerated at 4 ^{o}C. The supernatant from these samples was tested for fluorescence at the 490 nm excitation wavelength. This was converted back to fluorescein concentration in the supernatant by comparing fluorescence against a calibration curve prepared using fluorescein diluted to 0.125, 0.25, 0.5, 0.75, and 1 mg/L in distilled water. Fluorescein concentration in the floc was calculated by subtracting the final fluorescein concentration in the supernatant from the starting fluorescein concentration, multiplying by the volume of the initial solution and dividing by the mass of humic acid or kaolin present in the initial solution. An adsorption isotherm was then prepared by plotting fluorescein concentration in the floc by the final fluorescein concentration in solution.

RESULTS AND DISCUSSION

ZETA POTENTIAL MEASUREMENTS

Starting zeta potential of the humic and kaolin solutions at different starting concentrations in distilled water are shown in Figure 1(a). Humic acid solutions were typically around -800 mV while the kaolin solutions were around -550 mV. The volume of alum solution required to reduce zeta potential to zero was largely proportional to humic acid concentration while for kaolin it was proportional up to 80 mg/L kaolin concentration increasing between the 80 to 100 mg/L kaolin concentration range (Figure 1(b)). Al^{3+} dose ranged between 0.14 g to 0.2 g per g humic acid and between 0.07 g to 0.14 g per g kaolin. The zeta potential behaviour can be expected due to the different chemical structures of kaolin and humic acid as described below.

Kaolin is a 1:1 layered silicate mineral with one tetrahedral (T) sheet of silica (SiO_4) linked by the oxygen atoms to one alumina octahedral (O) sheet (AlO_6). These layers are bonded in stacks by hydrogen bonding between the oxygen on the outer face of the T sheet and the hydroxyl on the outer face of the O sheet on the next layer. The particles are typically plate like with the disc size 5–10 times larger than the thickness and possesses an overall negative on the surface due to isomorphous substitution of Si^{4+} for Al^{3+}, but a positive charge around the edges at low pH and negative at high pH due to protonation and deprotonation of exposed hydroxyl groups, with an isoelectric point around pH 7 (Ma and Eggleton 1999, Greenwood et al 2007). Cation exchange capacity of kaolin depends on the source of kaolin, particle size and pH and ranges between 0.028 meq/kg for well-ordered kaolin to 0.34 meq/kg for poorly ordered kaolin (Ma and Eggleton 1999) to 35-55 meq/kg (Kahr and Madsen 1995). CEC from the zeta potential measurements was calculated by multiplying the volume of alum solution added by the concentration of alum, dividing by the molecular weight of alum, multiplying

by the charge of Al^{3+} (3) and number of moles of Al^{3+} per alum molecule (2), and dividing by the mass of kaolin added to the solution, and it was found to be in the range of 10 to 16 meq/kg kaolin.

Figure 1: (a) Starting zeta potential of the humic and kaolin solutions at different starting concentrations (b) Volume of 1 g/L alum solution required to reduce zeta potential of 400 ml solutions to zero.

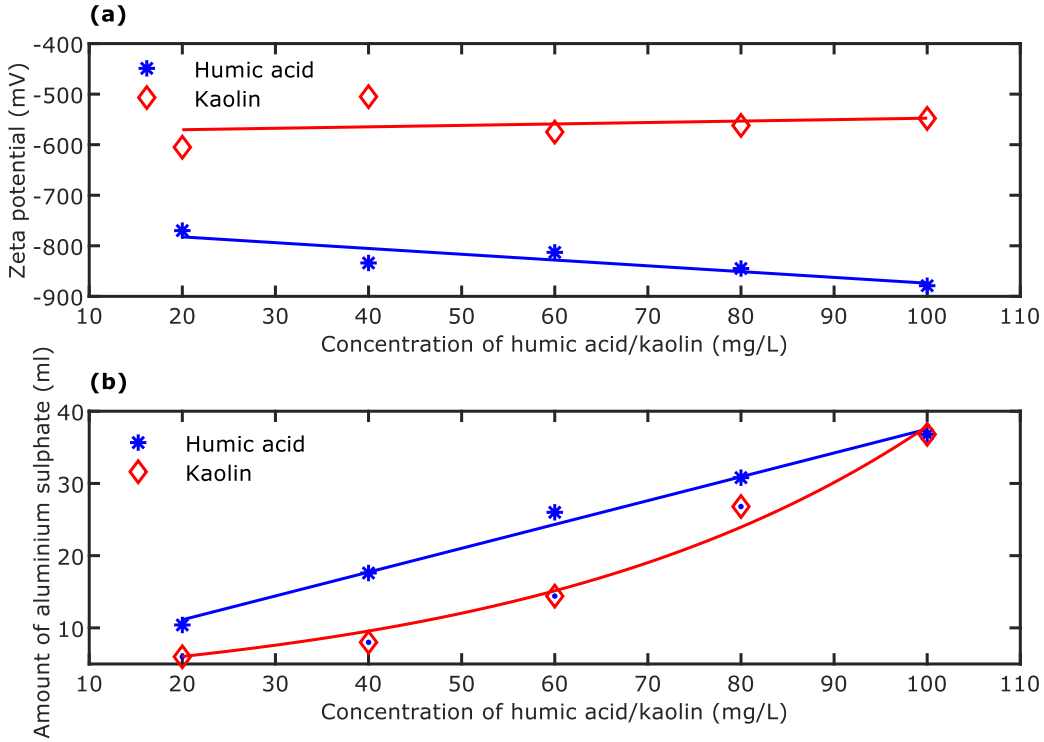

Humic acid is a large organic structure formed from the decomposition of biomass in soil, peat, coal and sediments, consisting of quinone, phenols, catechol and sugar moieties, with the phenolic and carboxylic groups readily forming complexes with cations such as magnesium, calcium, ferrous and ferric ions (de Melo et al.,2016)). CEC of humic acid was calculated to be between 16 to 23 meq/kg humic acid, greater than that of kaolin, as was demonstrated by humic acid's larger zeta potential.

TURBIDITY, PH AND PARTICLE SIZE MEASUREMENTS

Turbidity in humic acid and kaolin prior to flocculation increases with increased concentration as expected (Figure 2a), kaolin has a higher turbidity range from 9.2 to 139 NTU compared to humic acid with 1.1 to 72.9 NTU. This is likely due to kaolin clay sheet layers hydrating and exfoliating into disc shaped particles, while humic acid would completely dissolve. Turbidity of the solutions decreased after

flocculation showing a 25% to 82% removal of turbidity for humic acid and a 40% to 72.6% removal for kaolin between 60 to 100 mg/L concentrations.

Using a buffered solution (pH 7) resulted in a much lower removal of kaolin compared to unbuffered solution (pH 4–6.5 – Figure 3), and generally turbidity and pH of the flocculated kaolin solutions increased as fluorescein increased (Figure 2 and 3). The pH increase from fluorescein addition is from the sodium bicarbonate added to the stock fluorescein solution to get the fluorescein to dissolve. Kaolin has an isoelectric point at pH 3 – 4 and its zeta potential becomes more negative as pH increases (Dwari and Mishra, 2019), hence more alum is required to flocculate it. In addition, the charge of fluorescein is pH dependent (Le Guern et al. 2020), exhibiting a positive charge at pH 2.1 or less, a neutral charge between pH 2.1 and 4.3, a single negative charge between pH 4.3 to 6.4, and two negative charges above pH 6.4. Therefore, as more fluorescein solution is added, the pH charge results in a greater negative charge on the fluorescein as well as on the kaolin requiring more alum to neutralise the charge and give better flocculation.

In the case of humic acid, using a buffered solution gave a lower turbidity than an unbuffered solution. Humic acid also has an isoelectric point between pH 2-4 and becomes more negative as pH increases. However, the structure of humic acid consists of quinone, phenols, catechol and sugar moieties, similar to the chemical structure of fluorescein, hence interactions between the aromatic groups of the fluorescein and humic acid as well as hydrogen bonding will play an important role and appears to be more favourable at pH 6.9 than at the unbuffered pH of 3.97 to 6.24.

Particle size after flocculation in unbuffered humic acid and kaolin solutions generally decreased with increasing humic acid and kaolin concentrations (Figure 4a) and coincides with the increase in turbidity observed for the same conditions in Figure 2a. This is due in part to an increase in solution pH (Figure 3a) resulting in a more negative zeta potential for humic acid and kaolin requiring more alum for flocculation. In addition, the ratio of fluorescein to humic acid and kaolin decreases; it appears from Figure 4b that as fluorescein concentration increases (i.e. the ratio of fluorescein to humic acid and kaolin increases) particle size increases for kaolin, while humic acid as the largest particle size at a fluorescein concentration of 0.5 to 0.7 mg/L, hence fluorescein is contributing to some extent as a flocculant.

Figure 2: Turbidity measured in for (a) flocculated and unflocculated solutions at different concentrations of humic acid and kaolin and 0.48mg/L fluorescein (b) flocculated solutions of buffered and unbuffered 60 mg/L humic acid and kaolin solutions at different fluorescein concentrations.

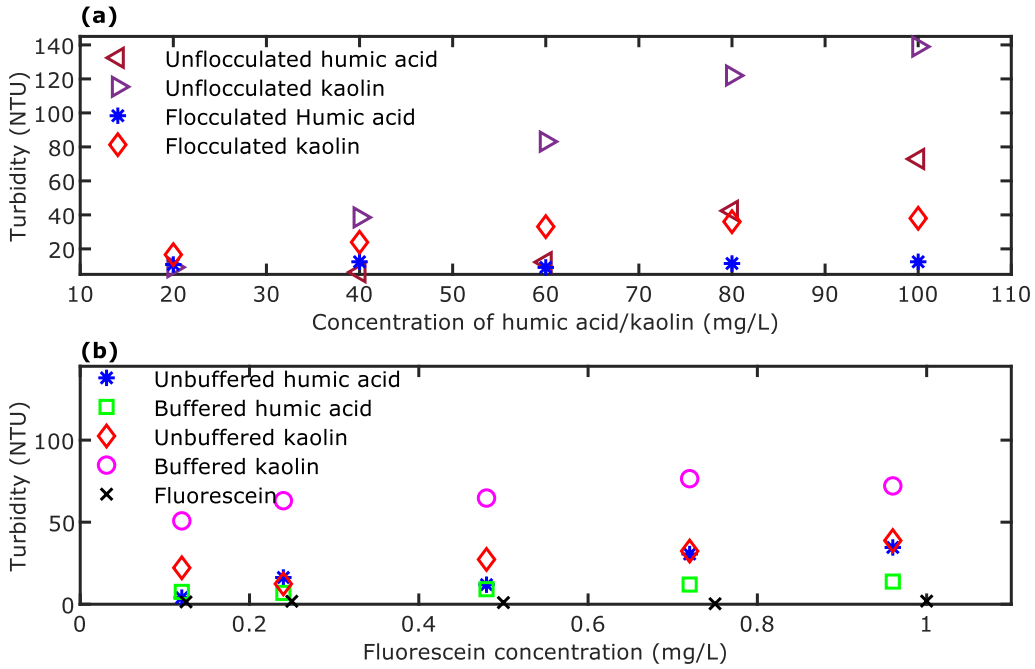

Figure 3: pH measurements for (a) flocculated solutions at different concentrations of humic acid and kaolin and 0.48mg/L fluorescein (b) flocculated solutions of buffered and unbuffered 60 mg/L humic acid and kaolin solutions at different fluorescein concentrations.

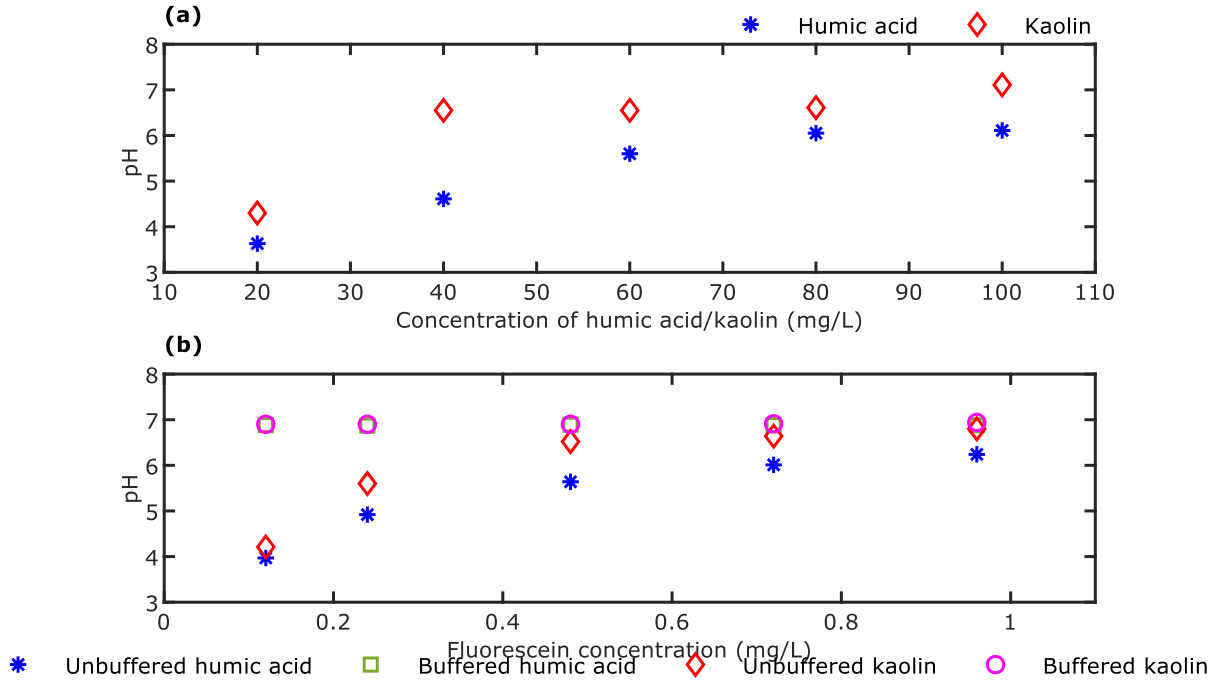

Figure 4: Particle size measurements for (a) unbuffered flocculated solutions at different concentrations of humic acid and kaolin and 0.48 mg/L fluorescein (b) buffered flocculated solutions 60 mg/L humic acid and kaolin solutions at different fluorescein concentrations.

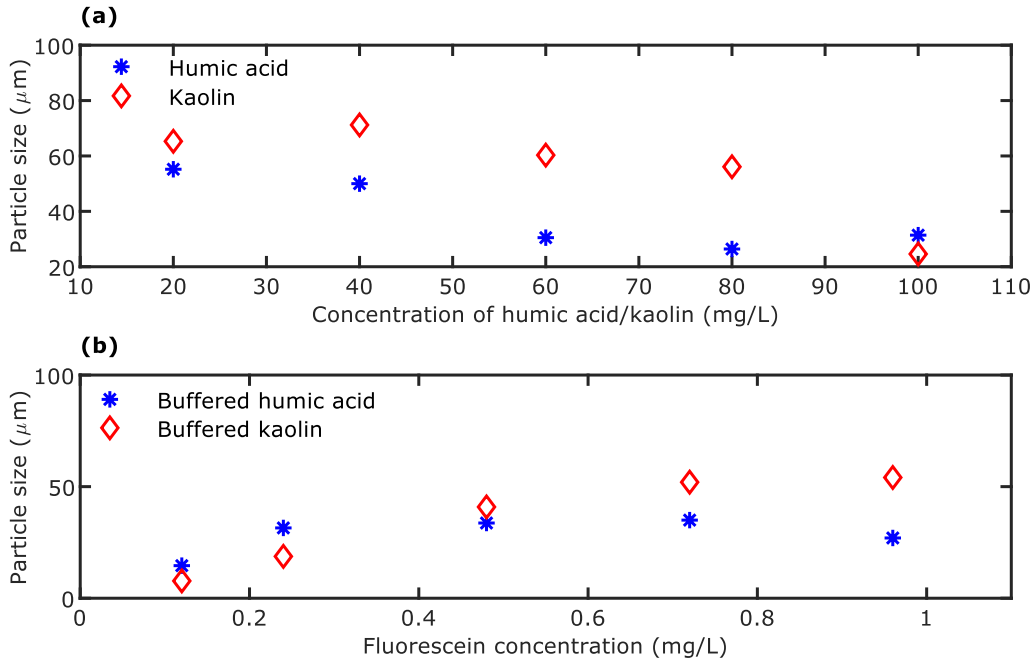

FLOC MORPHOLOGY

Observation of the floc particles under a light microscope showed kaolin floc particles are largely non spherical and flat, with the one observed in the image 222 to 223 μm in size (Figure 5) Humic acid flocs flocculated from with 20 mg/L to 40 mg/L humic acid solutions (i.e. a high ratio of fluorescein to humic acid) were non-spherical and flat, while the higher concentrations of humic acid (i.e. a low ratio of fluorescein to humic acid) resulted in floc particles with a more dense spherical shape (also as seen in Figure 4a). This suggests that fluorescein plays a role in bridging floc resulting in a larger floc (as seen in Figure 4b) and more flat, less spherical appearance. This has important implications for using fluorescein as a fluorophore as at high ratios of fluorescein to particulate and dissolved matter results in morphological changes to the floc which will impact on the interpretation of fluorescence data from floc particles. Ideally a fluorescein dose needs to be low enough to maintain a floc morphology similar to what would normally occur, but high enough to generate a fluorescence emission signal so light penetration of the floc can be accurately measured.

Figure 5: Microscope images (20x magnification) of kaolin floc particles from 20 mg/L unbuffered kaolin solutions with 0.48mg/L fluorescein.

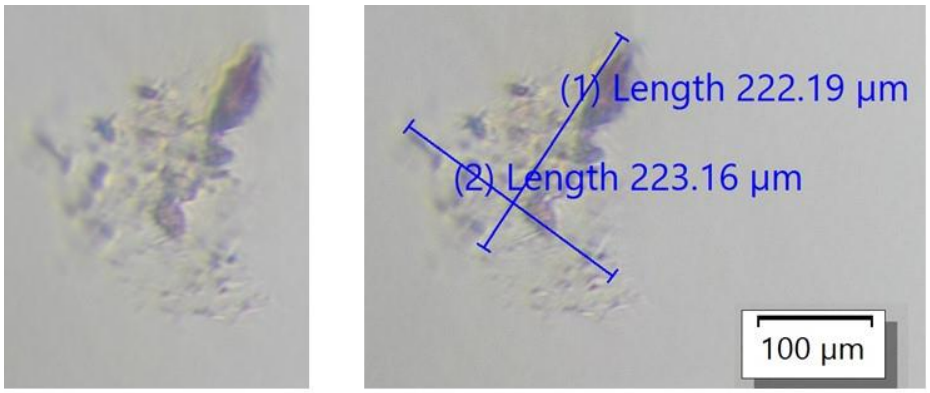

Figure 6: Microscope images (20x magnification) of humic acid floc particles from (a) 20 mg/L, (b) 40 mg/L, (c) 60 mg/L and (d) 80 mg/L, unbuffered humic acid solutions with 0.48mg/L fluorescein.

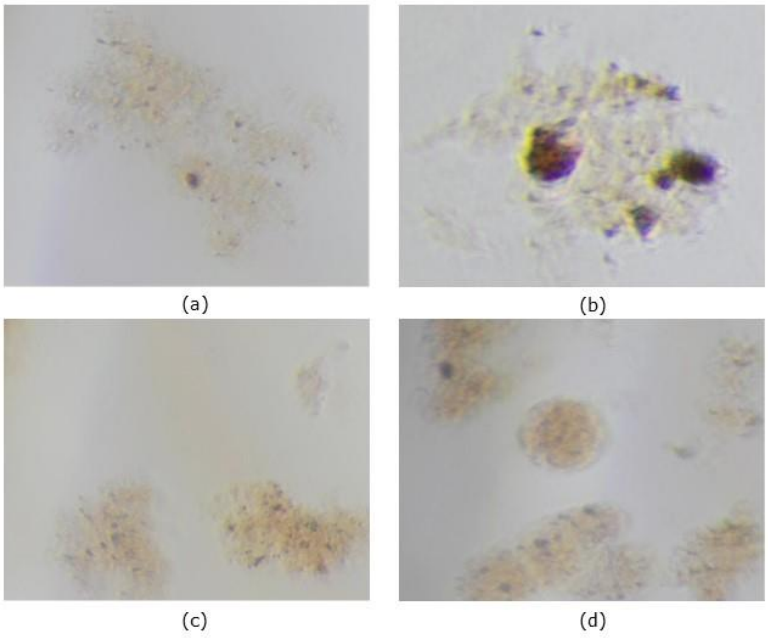

FLUORESCENCE MEASUREMENTS

Fluorescein fluoresces at excitation wavelengths between 250 nm to 330nm and 450 to 520 nm peaking at the 510 nm emission wavelength, when excited at 260 nm and 490 nm (Figure 7). This shows that fluorescein can be used for measuring UV penetration as well as visible light penetration and the fluorescence is at a significantly different wavelength to the wavelength used to excite the fluorophore. In addition, the emission from fluorescein when excited at 490 nm is approximately 80% of that emitted when excited at 260 nm, therefore excitation at visible wavelengths is a reasonable proxy for measuring fluorescence at the wavelengths used for UV disinfection. The accuracy of measurements will depend on the absorbance spectrum of the material the floc is made from (in addition, some materials are auto-fluorescing, e.g. chemical and protein structures

containing aromatic groups such porphyrins, tyrosine and tryptophan), but this can be measured using EEM and correcting for the differences in emission at the different wavelengths.

Figure 7: Fluorescence emission data for fluorescein at 0. mg/L in distilled water.

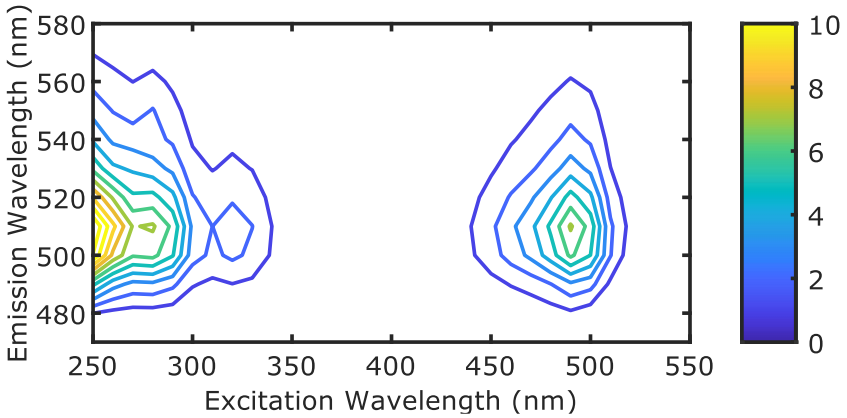

As kaolin and humic acid concentrations were increased a scattering effect in the fluorescence data was observed shown by first and second order Rayleigh scattering (Figure 8) (Cia et al., 2011; Tan et al., 2020), and a reduction in fluorescence emissions. The scattering is due to the flocculated material scattering the light as observed by the emission wavelength matching the excitation wavelength for first order, and the second order scattering due to the excitation light diffracting off the monochromator, passing through the sample and scattering as well, both of which become observable as the fluorescence emission decreases due to the equipment autoscaling the signal received. Scattering is stronger with kaolin because it is white and more reflective, while humic acid has a brown/black colour, is more absorbing, and exhibits a fluorescence signal at the 250-280 nm excitation wavelength due to the abundance of aromatic groups in its structure (termed auto-fluorescence, see Ma et al. 2017).

To examine the effect of fluorescein on fluorescence and scattering, another study was carried out using 60 mg/L kaolin and humic acid samples at different concentrations of fluorescein. As fluorescein concentration increases, the scattering effect is reduced and is barely observable at the 1 mg/L fluorescein concentration. The auto-fluorescence of humic acid is observed in Figure 9 for the sample with 0 mg/L fluorescein as the sample does not have fluorescein in it. To generate a reasonable fluorescence signal, kaolin needs at least 1 mg fluorescein per 60 mg of kaolin, while humic acid needs 0.72 mg fluorescein per 60 mg humic acid.

Figure 8: Fluorescence emission data for flocculated solutions containing different concentrations of kaolin and humic acid and 0.5 mg/L fluorescein.

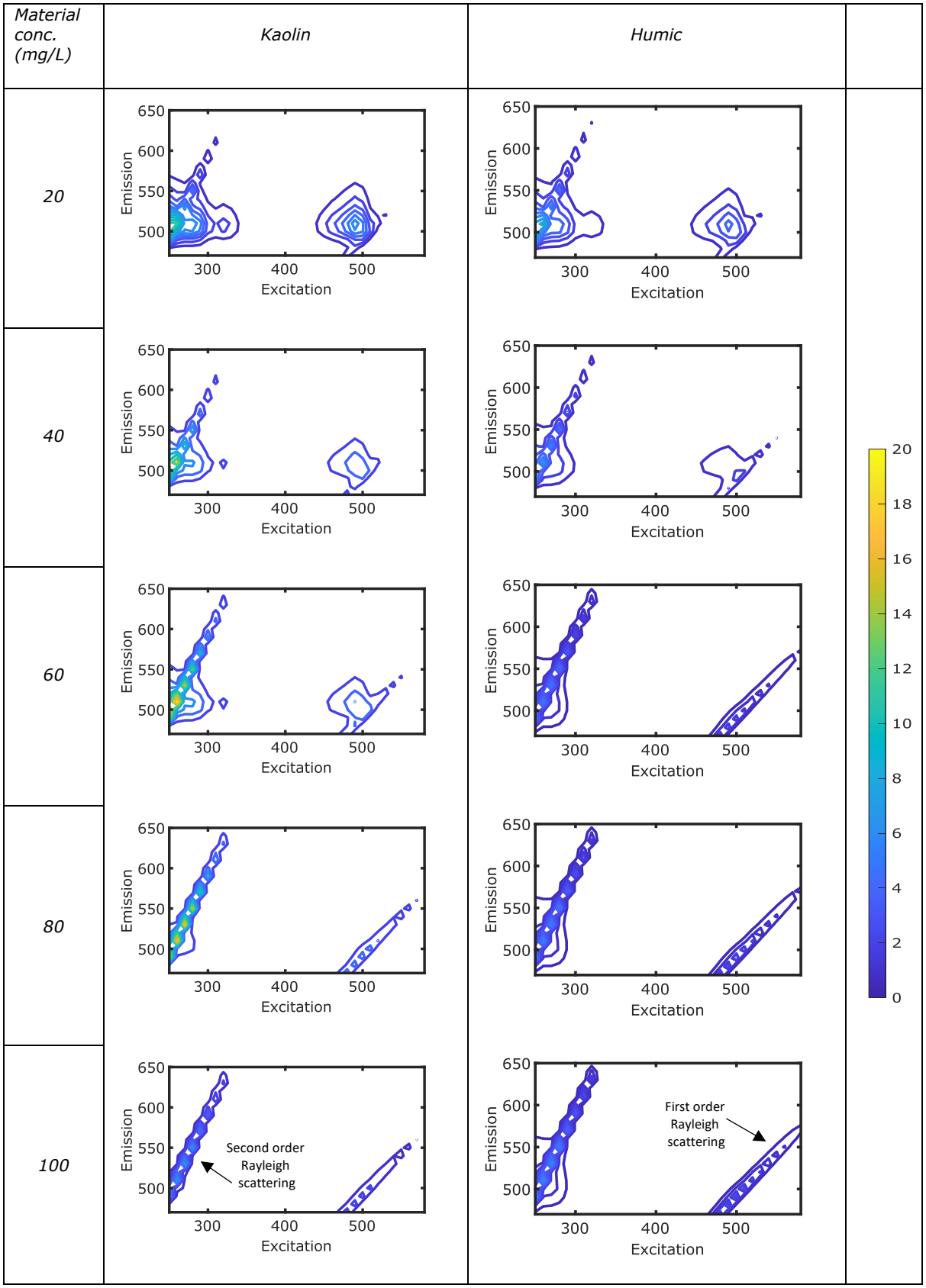

Figure 9: Fluorescence emission data for flocculated solutions containing different concentrations of fluorescein in 60 mg/L of kaolin and humic acid.

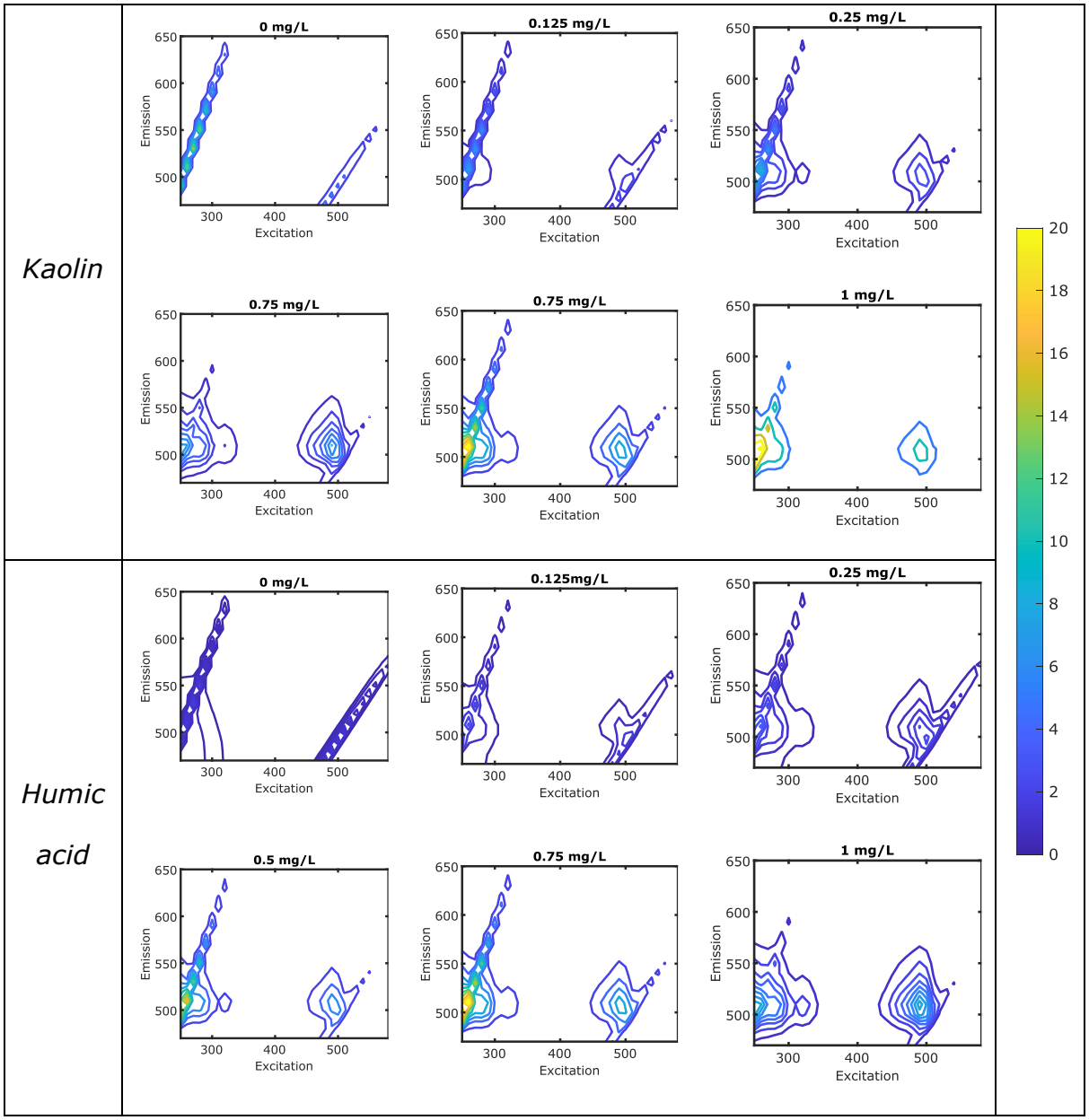

FLUORESCEIN ADSORPTION RESULTS

Fluorescence of samples can come from free fluorescein in solution and from bound fluorescein in the floc. Ideally, most of the fluorescein should be bound in the floc to generate reliable light penetration data for the floc from fluorescence measurements. To examine the extent of adsorption of fluorescein into floc samples of buffered flocculated humic acid and kaolin solutions were centrifuged to remove the floc particles and fluorescence of the supernatant was measured. Fluorescence data was compared against a calibration to determine fluorescein concentration in solution, and by mass balance the concentration of fluorescein in the floc, which was then used to generate adsorption isotherms (Figure 10). The

isotherms were non-linear and unfavourable, i.e. fluorescein had a low affinity for humic acid and kaolin flocs and predominantly resided in solution at low fluorescein concentrations. Fluorescein adsorption was greater on kaolin than on humic acid reaching a concentration of 4 mg/g kaolin and 0.35 mg/g on humic acid. Out of the isotherm models applied, the Henry and Langmuir isotherms gave the worst fits, while the Freudlich isotherm:

$$Q = KC^{1/n} \quad (1)$$

(where Q is the adsorbed amount at equilibrium, K is the adsorption capacity and $1/n$ is adsorption intensity) gave the best fit for kaolin solutions (Figure 10 (a)). Freundlich isotherm model parameters were determined using the least squares curve fitting method in Matlab and were found to be K =7.094 and n =0.515.

The SIPs isotherm:

$$Q = \frac{K'C^{\beta}}{1 + \alpha C^{\beta}} \quad (2)$$

(where Q is the adsorbed amount at equilibrium, β is a model exponent and α and K' are model constants respectively (Kalam et al.,2021)), gave the best fit for humic acid solutions (Figure 10(b)). SIPS model parameters are K' = 1.975, α = 7.257 and β = 3.51.

Figure 10: Fluorescein adsorption isotherm for flocculated samples using (a) 60 mg/L kaolin and (b) 60 mg/L humic acid.

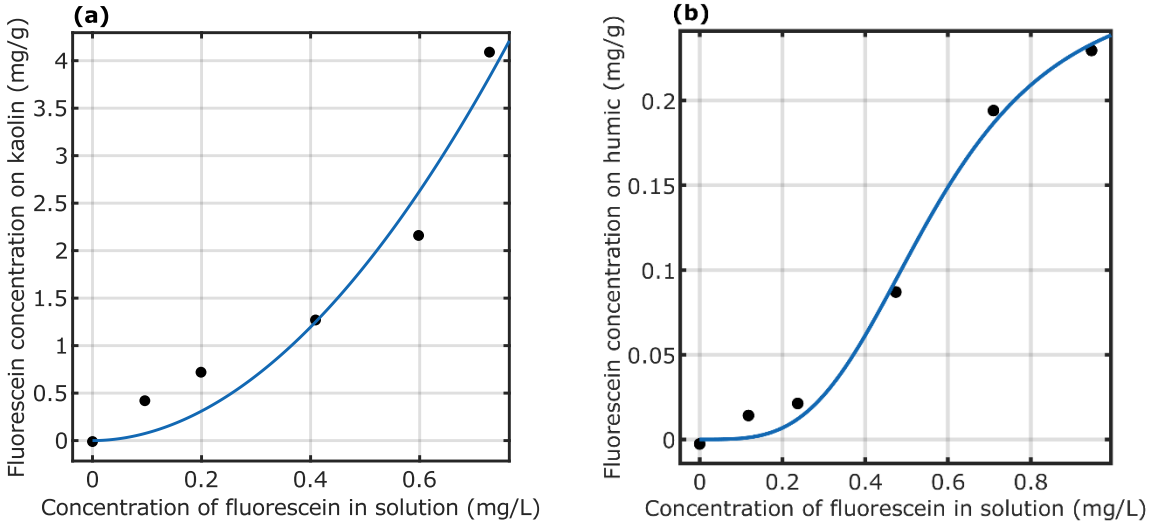

Ideally, the adsorption isotherm should be Langmuir, i.e. the fluorescein has a high affinity for humic acid and kaolin and will be present in high concentrations on the floc, even at low concentrations in solution. Based on previous findings for turbidity, pH and particle size and explanations provided, both kaolin, humic acid and fluorescein have a negative charge at the conditions used and the alum doses used were not high enough to promote good flocculation. Therefore, more trials will be conducted at higher alum concentrations (or using different flocculants) to promote good floc formation and good incorporation of fluorescein into the floc.

CONCLUSIONS

In this study, fluorescein was used to measure fluorescence of floc particles made from humic acid and kaolin using alum as flocculant. Fluorescein improved floc particle size and changed floc morphology from a dense spherical floc to a flat non-spherical shape. Floc particles exhibited Rayleigh scattering that reduced in intensity as fluorescein concentration increased. Fluorescein emits at a similar intensity and wavelength when it is excited at 260 nm and 490 nm indicating that fluorescence using visible light is a good proxy for measuring fluorescence using UV light (depending on the light absorbance spectrum of the material the floc is prepared from). Greater alum doses need to be used to improve flocculation and fluorescein incorporation into floc.

ACKNOWLEDGEMENTS

The authors thank AHEAD project for providing financial assistance for three years to support the study.

REFERENCES

Augsburger, N., Rachmadi, A. T., Zaouri, N., Lee, Y., and Hong, P. Y. (2021). Recent update on UV disinfection to fulfill the disinfection credit value for enteric viruses in water. Environmental Science & Technology, 55(24), 16283-16298.

Cao, B., Gao, B., Xu, C., Fu, Y., & Liu, X. (2010). Effects of pH on coagulation behavior and floc properties in Yellow River water treatment using ferric based coagulants. Chinese Science Bulletin, 55, 1382-1387.

Cantwell, R. E., Hofmann, R., & Templeton, M. R. (2008). Interactions between humic matter and bacteria when disinfecting water with UV light. Journal of applied microbiology, 105(1), 25-35.

Chen, P., Liu, S., Liu, Z., Hu, X. (2011) Study on the ternary mixed ligand complex of palladium (ii)–aminophylline–fluorescein sodium by resonance rayleigh scattering, second order scattering and frequency doubling scattering spectrum and its analytical application. Spectrochimica Acta Part A: Molecular and Biomolecular Spectroscopy 78(1), 518–522.

de Melo, B. A. G., Motta, F. L., & Santana, M. H. A. (2016). Humic acids: Structural properties and multiple functionalities for novel technological developments. Materials Science and Engineering: C, 62, 967-974.

Dwari, R. K., & Mishra, B. K. (2019). Evaluation of flocculation characteristics of kaolinite dispersion system using guar gum: a green flocculant. International Journal of Mining Science and Technology, 29(5), 745-755.

Emerick, R. W., Loge, F. J., Ginn, T., & Darby, J. L. (2000). Modeling the inactivation of particle-associated coliform bacteria. Water Environment Research, 72(4), 432-438.

Greenwood, R., Lapčíková, B., Surýnek, M., Waters, K., & Lapčík, L. (2007). The zeta potential of kaolin suspensions measured by electrophoresis and electroacoustics. Chemical Papers, 61(2), 83-92.

Gregory, J. J. (2005). Particles in water properties and processes. London: Boca Raton, FL:IWA Pub. ; Taylor & Francis.

Kalam, S., Abu-Khamsin, S. A., Kamal, M. S., & Patil, S. (2021). Surfactant adsorption isotherms: A review. ACS omega, 6(48), 32342-32348.

Kawahigashi, M., Sumida, H., & Yamamoto, K. (2005). Size and shape of soil humic acids estimated by viscosity and molecular weight. Journal of colloid and interface science, 284(2), 463-469.

Key, J. A., Koh, S., Timerghazin, Q. K., Brown, A., & Cairo, C. W. (2009). Photophysical characterization of triazole-substituted coumarin fluorophores. Dyes and Pigments, 82(2), 196-203.

Kahr, G. & Madsen F. T. (1995). Determination of the cation exchange capacity and the surface area of bentonite, illite and kaolinite by methylene blue adsorption. Applied Clay Science, 9, 327-336.

Kollu, K. and Örmeci, B. (2012) Effect of particles and bioflocculation on ultraviolet disinfection of Escherichia coli. Water research, 46(3), pp.750-760.

Lakowicz, J. R. (2006). Principles of fluorescence spectroscopy (3rd ed.). New York: Springer.

LeChevallier, M.W. and Au, K.K. (2004) Water treatment and pathogen control. Iwa Publishing.

Le Guern, F., Mussard, V., Gaucher, A., Rottman, M., & Prim, D. (2020). Fluorescein derivatives as fluorescent probes for pH monitoring along recent biological applications. International Journal of Molecular Sciences, 21(23), 9217.

Li, W., Qi, W., Chen, J., Zhou, W., Li, Y., Sun, Y., & Ding, K. (2019). Effective removal of fluorescent microparticles as Cryptosporidium parvum surrogates in drinking water treatment by metallic membrane. Journal of Membrane Science, 117434.

Long Term 2 Enhanced Surface Water Treatment Rule (Vol. Parts 141 and 142; Standard). (2010, April). Washington, DC 20460-0001: U.S. Environmental Protection Agency.

Ma, C. H. I., & Eggleton, R. A. (1999). Cation exchange capacity of kaolinite. Clays and Clay minerals, 47, 174-180.

Ma, J., Fu, K., Jiang, L., Ding, L., Guan, Q., Zhang, S., ... & Fu, X. (2017). Flocculation performance of cationic polyacrylamide with high cationic degree in

humic acid synthetic water treatment and effect of kaolin particles. Separation and Purification Technology, 181, 201-212.

Pang, L., Nowostawska, U., Ryan, J. N., Williamson, W. M., Walshe, G., & Hunter, K. A. (2009). Modifying the surface charge of pathogen-sized microspheres for studying pathogen transport in groundwater. Journal of Environmental Quality, 38(6), 2210-2217.

Rossle, N. F., and Latif, B. (2013) Cryptosporidiosis as threatening health problem: a review, Asian Pacific journal of tropical biomedicine, 3 (11), 916-924.

Singh, P., Gupta, R., Sinha, M., Kumar, R., & Bhalla, V. (2016). MoS 2 based digital response platform for aptamer based fluorescent detection of pathogens. Microchimica Acta, 183, 1501-1506.

Tan, L., Du, W., Zhang, Y., Tang, L. J., Jiang, J. H., & Yu, R. Q. (2020). Rayleigh scattering correction for fluorescence spectroscopy analysis. Chemometrics and Intelligent Laboratory Systems, 203, 104028.

Templeton, M.R., Andrews, R.C. and Hofmann, R. (2005) Inactivation of particle-associated viral surrogates by ultraviolet light, Water research, 39(15), pp.3487-3500.